Synchronous machine faults detection and isolation for electro-mechanical actuators in aeronautics

Garance Vinson, Michel Combacau, Thomas Prado

▶ To cite this version:

HAL Id: hal-00925501

https://hal.science/hal-00925501

Submitted on 9 Jan 2014

Synchronous Machine Faults Detection and Diagnosis for Electro-mechanical Actuators in Aeronautics

Garance Vinson * Michel Combacau ** Thomas Prado ***

* CNRS LAAS, 7 av du Colonel Roche, Univ de Toulouse, LAAS-UPS, 31400 Toulouse, France and Messier-Bugatti-Dowty, 78140 Velizy-Villacoublay, France (Tel: +33-146-29-8343, e-mail: garance.vinson@safranmbd.com).
** CNRS LAAS, 7 av du Colonel Roche, Univ de Toulouse, LAAS-UPS, 31400 Toulouse, France (e-mail:combacau@laas.fr)
*** Messier-Bugatti-Dowty, 78140 Velizy-Villacoublay, France (e-mail: thomas.prado@safranmbd.com)

Abstract: The reported work is the design of a Fault Detection and Isolation system for permanent magnet synchronous machine (PMSM). Two main faults occurring on these machine are identified as inter-turns short-circuit and rotor single pole demagnetization, and characterized. An analytical model of synchronous machines is developed and simulated using Matlab Simulink. This model allows simulating nominal and faulty motor behaviour. It is parameterizable and is able to simulate several stages of the two degradation. Specific indicators are proposed for each fault. They do not require additional material or sensors since they are based on the signals already monitored for the machine control. To illustrate the method an application is made on an innovative 12-slots 10-poles PMSM that becomes more and more popular in aeronautics, and on a 9-slots 8-poles PMSM used in critical application as braking.

Keywords: Fault detection, Electro-mechanical application, Health-Monitoring, Aeronautics, Short-circuit, Permanent Magnet Synchronous Machine, Diagnosis.

1. INTRODUCTION

Facing the growth of the air transport demand, the environmental issues and the competition between aircraft manufacturers, the aerospace industry is looking for safer, cleaner and cheaper aircrafts. Beside the major step changes occurring in engines, structures and aerodynamics, improvement of efficient secondary power systems offers promising advances. In this area, flight control and landing gears actuation appear as major power consumers that makes them a key driver for the sizing of the redundant aircraft power networks. As power is conveyed without mass transfer with electrical wires, power-by-wire has evident advantages against pneumatic or hydraulic power distribution.

The electrification of aeronautical actuation systems is linked to another concern of Aircraft manufacturers. Indeed requirements are increasing regarding operational availability of equipment and a more efficient management of the maintenance. To achieve this, two families of solution can be combined: during design with the development of fault tolerant or fault resistant components, and during operational life with health monitoring. This latest appears as a very promising solution. However, implementing mature health monitoring features cannot be achieved without significantly improving the knowledge of the components wear and failures to enable proposing solutions for early fault detection, diagnosis and prognosis.

This paper specifically deals with FDI (fault detection and isolation). This process consists in (1) the detection of an abnormal behaviour of the system under study and (2) the identification of the fault, this last task dwells in identifying which component is involved and what fault occurred at which level. It determines the health of the system and its components.

FDI's basic principle is to compare the real behaviour of the system with the expected behaviour that comes from a system model. Comparison is firstly made with the model of nominal operation during the detection stage. If there is a difference between observed and simulated nominal behaviours, then identification process takes place and comparison is done with faults models. To assess the consistency between real and expected behaviours, indicators are used. These indicators are based on the information available on the system e.g. on the observations coming from the sensors. For each fault, a battery of indicators is used whose values vary in a well-known way when the fault occurs; this is the fault signature. This signature is identified from a model of the system including faults models. This model might be analytical, numerical, or both, depending on the knowledge available on the faulty system.

The reported work is the design of a FDI system for PMSM and the application on two types of machines, a 12-slots 10-poles synchronous machine and a 9-slots 8-

poles used in safe critical aerospace actuation, e.g. for landing gear extension and retraction or for brakes. First the context of the study and the needs will be described. Second the two main faults occurring on PMSM will be identified and characterized. Third detection and diagnosis will be discussed. Finally a conclusion will summarize the contribution and point out plans for future work.

2. ISSUE PRESENTATION

2.1 The 12-slots 10-poles and 9-slots 8-poles synchronous machines

In the domain of PMSM, modular topology becomes more and more popular [Nierlich]. The two studied machines are 3-phases radial flux machines with non-overlapped coils and surface mounted permanent magnet. In the 12-slots 10-poles PMSM coils are wound around a single tooth in the sequence [C+ B- A+ C- B+ A-].There are two sections repeating themselves with a negative periodicity. In the 9-slots 8-poles machine there are two coils a slot and they are wound in the sequence [A+ A- A+ B+ B- B+ C+ C- C+].

2.2 A generic PMSM model

No matter what the geometry of the PMSM is, their nominal behavior can be modelled as follows. Voltages induced in coils by the rotor E_a, E_b and Ec are a function of the rotor mechanical position. Induced voltages derive from magnetic flow, and magnetic flow induced in a single coil is modelled with the following hypotheses : no saturation, no magnetic leak in the magnetic circuit and uniform magnetic flow B_{max} induced by the magnet. A geometric analysis of the position of the magnet facing the coil leads to a fine approximation of the magnetic flow through the coil. Figure 1 shows the nominal magnetic flux in a given coil for the 10-12 motor. A harmonic analysis of
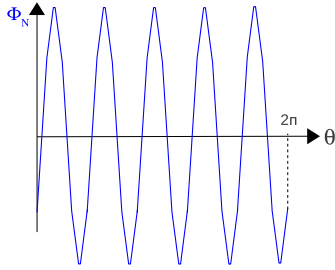

Fig. 1. Magnetic flux in a coil for the 10-12 PMSM

this waveform shows that it can be approximated by only the harmonic of rank five (this fundamental ranks depends on the number of poles). The induced voltages will then be considered to be sinusoidal. Coils are not surimposed so there are no mutual inductance between phases and phase to phase voltages are:

$$U_{ab} = R(I_b - I_a) + Ld(I_b - I_a)/dt + E_b - E_a \qquad (1)$$
$$U_{bc} = R(I_c - I_b) + Ld(I_c - I_b)/dt + E_c - E_b \qquad (2)$$
$$I_a + I_b + I_c = 0 \qquad (3)$$

where R is the phases resistance and L is the phases inductance. Currents and induced voltages produce an electromagnetical torque C_{em}.

$$C_{em} = (E_a I_a + E_b I_b + E_c I_c)/\Omega \qquad (4)$$

2.3 Health monitoring of the PMSM

The PMSM can be advantageously monitored to enable just in time maintenance, that is to say planning the maintenance action right before the failure. In the reported work, a supervision system is designed. It consists in 2 modules: (1) a detection module warning when the machine does not operate properly, and (2) a diagnosis module isolating the fault.

The first step of the FDI system design is to choose which particular faults need to be monitored. For this purpose both frequency and gravity of all the possible machine faults are evaluated through in-service experience, tests, reliability analysis, and experts' judgement. Fault frequency and gravity allow assessing their criticality. Faults are then ranked with respect to criticality. Sudden faults are dismissed of the present study while only the progressive faults remain considered as they let time to develop a maintenance strategy before the machine fails. This choice is also obviously a step towards the prognosis stage. The most critical faults that are addressed here are inter-turns short-circuit and permanent magnet demagnetization. Next step is to characterize these faults to be able to detect, isolate, and as expected prevent them. This is the purpose of next chapter.

3. FAULTS CHARACTERIZATION

3.1 Inter-turns short-circuits

Winding turn's insulation is degraded by various causes like high temperatures variations, and high voltage rates due to PWM (pulse width modulation) inverter fed. This insulation degradation comes finally to inter-turns short-circuit. Inter-turns short-circuits diminish the number of active turns in the affected phase, which then produces a smaller electromotive force. This leads to unbalanced statoric flux. It also creates a current loop, often called short-circuit loop. The current flowing in this loop can be pretty high leading to irreversible damages in the all system. For this reason, early detection of this fault is of particular importance since it may lead to the complete destruction of the phase which will severely affect the machine performance.

Some authors as Cardoso et al. (1999), perform FDI based on experimental results only. This can become very expensive if one wants the results for several degradation stages. In addition this approach cannot be generalized to other systems without any deeper theoretical study. That is why the author has chosen a model-based FDI. To gain knowledge on the machine behaviour during inter-turns short-circuits, an analytical fault model is built. It is then simulated using Matlab Simulink as a time domain simulation tool. Insulation fault is represented with a variable resistor connecting two points of the coil as in Khov (2009),Vaseghi (2009), and Trigeassou (2011).

The model is represented in figure 2, U_{ab}, U_{bc}, U_{ca} are the power supply voltage, E_{a1}, E_{a2}, E_b, E_c are the windings induced voltage, L_a, R_a, L_b, R_b, L_c, R_c are the phase inductance and resistance, I_a, I_b, I_c are the phase current,
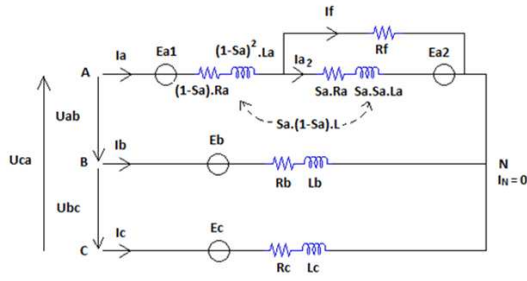
Fig. 2. A-phase inter-turns short-circuit model

I_f is the current flowing in the short-circuit loop, $I_N = 0$ means that there is no neutral current and the sum of the three phase currents is nul.

Two other parameters are involved, representing the fault severity. First, R_f represents the resistance of the turns insulator at the point of short-circuit, that varies between 1000 ohm typically for a healthy insulator and 0 ohm for a direct short-circuit with a hole in the insulator. Second, Sa represents the percentage of turns short-circuited in A-phase.

The short-circuit loop equation gives:

$$I_f = I_a(S_aR + (S_a^2L - M_a)j\omega)/(R_f + S_aR + S_a^2Lj\omega) \\ + E_aS_a/(R_f + S_aR + S_a^2Lj\omega) \qquad (5)$$

Equation (1) becomes:

$$U_{ab} = ZI_b + E_b - Z_a'I_a - (1 - S_a - Z_{ea})E_a \qquad (6)$$

with

$$Z_{ea} = S_a(R_f + j\omega M_a)/(R_f + S_aR + S_a^2Lj\omega) \qquad (7)$$

and

$$Z_a' = (1 - S_a)R + j\omega(1 - S_a)^2L - j\omega M_a + \\ (R_f + j\omega M_a)(S_aR + (S_a^2L - M_a)j\omega) \\ /(R_f + S_aR + S_a^2Lj\omega) \qquad (8)$$

3.2 PM demagnetization

The rotor also receives many stresses. High short-circuits currents, field weakening operation, and high temperatures may demagnetize one or several poles of the rotor. This irreversibly decreases residual induction level of the magnets. One magnet may also be broken by centrifugal force or manufacturing default. Such a demagnetized pole creates a smaller induced voltage in the windings. This unbalances the rotor magnetic flux. Unlike inter-turns short-circuit, the effect is the same on every phase. This difference will allow efficient discrimination between one fault and the other.

To gain knowledge on the machine behaviour when a pole demagnetization occurs a fault model is built. It consists in adding a flux produced by a single magnet To model the demagnetization, we consider an additional negative flux induced by a single magnet. This additional flux can be adjusted within the range $[0, B_{max}]$ to simulate a partial or total demagnetization of a pole. Figure 3 shows this additional flow that mustbe added to to nominal (figure **??**) flow in the considered coil.
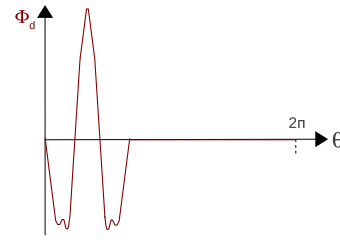

Fig. 3. Magnetic flux in a coil in case of 50% demagnetization of a magnet

This simplified model gives the same results as those obtained by simulation with an professional software based on a finite element model. A Matlab Simulink temporal model is built based on a steady-state model, developed using a design tool based on FE (finite element) calculation. This initial model outputs the magnetic flux repartition in case of demagnetization of the PMSM. The modeling activities contribution is to enable simulating a faulty PMSM with any numbers of poles instead of the two poles model often chosen for simplicity reason such as in [Farooq].
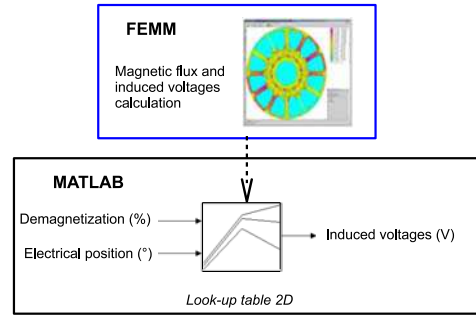

Fig. 4. Demagnetization model

Results are presented as a table giving induced voltage as a function of rotor position. Simulations are realized for 0 to 100% of one single pole demagnetization. Computation step is 1.6 degree on a total of 360 degrees for a complete rotor rotation, which means 225 points are computed for one turn.

In the dynamical model induced voltages are modelled with three look-up tables (figure 4). These look-up tables take electrical position and demagnetization percentage in input, and output induced voltage. Between the points computed with FEMM, values are linearly interpolated. This method allows combining the results precision of the finite element model and the high computing speed of the dynamic model.

4. FAULT DETECTION AND ISOLATION

In order to perform FDI, specific fault indicators have to be built. Common studies Penman et al. (1994), Casadei et al. (2009), design FDI systems with the help of electromagnetic flux sensors that is uneasy to implement on-board aircrafts. For this reason the proposed indicators must be based only on the available data coming from the existing sensors. The signals monitored for the motor control are phase currents and rotor vs stator angular position.

4.1 Inter-turns short-circuit indicators

The analytical study of the short-circuited electrical motor allows the author to build indicators based on phase currents.

Induced voltages have a $2\pi/3$ phase-shift, and so do phase voltages. E_b and U_{bc} are then expressed as: $E_b = E_a exp(j2\pi/3)$ and $U_{bc} = U_{ab}exp(j2\pi/3)$.

The relationship between phase currents can be expressed as: $I_b = X_b I_a$ and $I_c = X_c I_a$. In a healthy situation, the value of these coefficients are: $X_{bnom} = exp(j2\pi/3)$ and $X_{cnom} = exp(-j2\pi/3)$.

Induced voltages and phase to phase voltages are linked by the relations: $E_a = X_e U_{ab}, E_b = X_e U_{bc} and E_c = X_e U_{ca}$.

To find out the relationship between I_b and I_a. To do so I_a is expressed as a function of U_{ab} in two different ways. Firstly, equation (6) gives $I_a = Z_2 U_{ab}$ whith

$$Z_2 = (1 - (exp(j2\pi/3) - (1 - S_a - Z_{ea}))X_e) \tag{9}$$
$$/(ZX_b - Z_a')$$

Secondly, equation (2) gives $I_a = Z_3 U_{ab}$ whith

$$Z_3 = -(exp(j2\pi/3) + X_e + 2X_e.exp(j2\pi/3) \tag{10}$$
$$/(Z(1 + 2X_b)))$$

By solving $Z_2=Z_3$ the author finds X_b value which is the ratio between I_b and I_a:

$$X_b = (Z_a'exp((j2\pi)/3) - Z - ZX_e + Z_a'X_e$$
$$+ZX_e exp((j2\pi)/3) + 2Z_a'X_e exp((j2\pi)/3)$$
$$+S_a ZX_e - ZZ_{ea}X_e) \tag{11}$$
$$/(2Z + Zexp((j2\pi)/3) + 3ZX_e$$
$$-2S_a ZX_e + 2ZZ_{ea}X_e)$$

The relationship between I_c and I_a is then deduced from equation (3) which gives $X_c = -1 - X_b$.

Another interesting relationship is the one between the faulty current I_a and the healthy current I_{anom}. In healthy conditions, $I_{anom} = Z_1 U_{ab}$ with

$$Z_1 = (1 - (exp(j2\pi/3) - 1)X_e)/(Z(exp(j2\pi/3) - 1)) \tag{12}$$

I_a/I_{anom} is then known from equations (9) and (12) and the analytical form is given by $I_a/I_{anom} = Z_2/Z_1$.

Finally, the short-circuited loop current I_f is characterized as opposed to I_a. Indeed equation (5) leads to $I_f = X_f I_a$ with

$$X_f = (S_a R + (S_a^2 L - M_a)j\omega + S_a X_e/Z_2) \tag{13}$$
$$/((R_f + S_a R + S_a^2 Lj\omega))$$

All the currents I_b, I_c, I_f and I_{anom} are known from their relationship to I_a, and these relationships are a function of the short-circuit intensity characterized by R_f and S_a.

Dynamical simulations are run with Matlab Simulink. Figure 5 and 6 show the results of simulation of temporal evolution of phase currents. This simulation enhance the differences in phases and magnitudes of the three currents, which can be well pointed out by the Fresnel diagram.
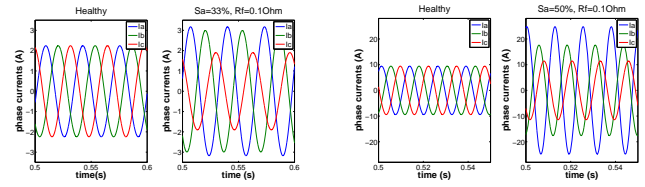

Fig. 5. Phase currents simulation results, with a healthy motor and a A-phase short-circuited motor, for the 9-8 PMSM (left) and the 10-12 PMSM (right).
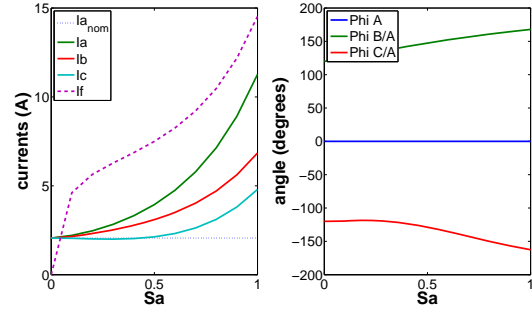

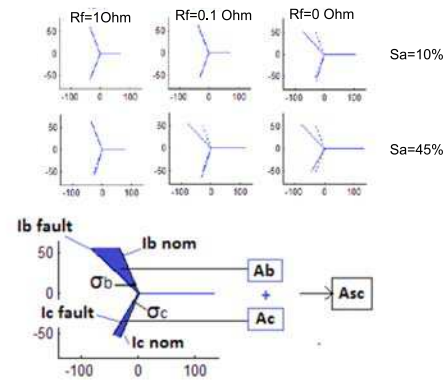Fig. 6. Evolution of phases and magnitudes of currents as a function of Sa for the 9-8 PMSM with Rf=0.1Ω.

Fig. 7. Fresnel diagram changes for several values of Sa and Rf, and calculation of the Asc indicator

Graphically it is easy to deduce that the sum of the areas of the two triangles formed by faulty and nominal phase currents I_b and I_c is an efficient candidate for inter-turn short-circuit indicator. This area is computed as in

$$A_{sc} = |I_{bn}I_{bf}sin(\sigma_b)| + |I_{cn}I_{cf}sin(\sigma_c)|, \tag{14}$$

Where I_n is the nominal current magnitude, I_f is the faulty current magnitude, and σ_b and σ_c are the angle between nominal phase shift $(2\pi/3)$ and faulty phase shift between A-phase and B or C-phase (figure 7).

Figure 8 swows variation of A_{sc} with R_f and S_a.

Stator temperature varies a lot during operationnal life which may modify phase resistance up to 20% of its nominal value. Tests are run to verify $A_{s}c$ robustness to phase resistance variation (Fig fig:robustesse).
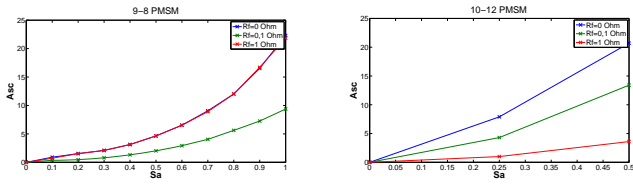
Fig. 8. Short-circuit indicator Asc as a function of the number of short-circuited turns Sa and of fault resistance Rf, for the 9-8 PMSM (left) and the 10-12 PMSM (right).
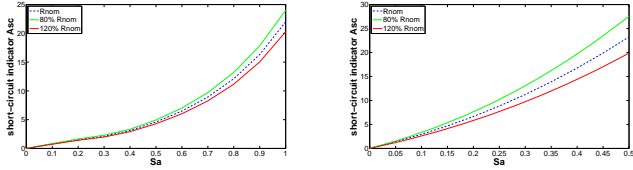

Fig. 9. Asc indicator robustness while the phase resistance changes from 80 to 120% of its nominal value due to stator temperature variation, for the 9-8 PMSM (left) and the 10-12 PMSM (right).

4.2 Demagnetization indicator

To model the demagnetization, we consider an additional negative flux induced by a single magnet. This additional flux can be adjusted within the range $[0, B_{max}]$ to simulate a partial or total demagnetization of a pole. An harmonic analysis of this additionnal flux shows several specific harmonics. These harmonics are seen in the three induced voltages which causes new harmonics in phase currents as well. An indicator can be build on these faulty harmonics for the demagnetization phenomenon (sum of their energy for instance).The most exploitable results are in the frequency domain, as already mentioned in [Ruschetti].

10-12 PMSM   Due to the motor configuration, the fundamental harmonics is the fifth one. New harmonics appear in faulty phase currents (H_1, H_7, H_{11}). This makes H_{dem}, defined as the sum of the amplitudes of all these new harmonics, a good candidate for a demagnetization indicator (figure 11).
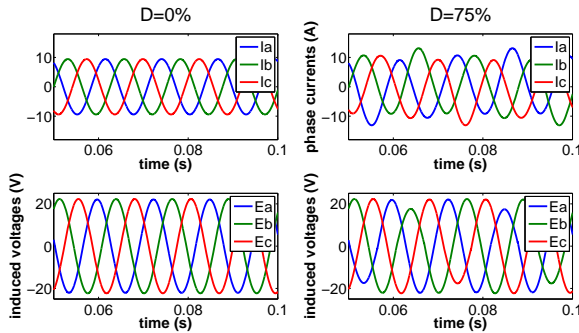

Fig. 10. Temporal evolution of the phase currents in case of demagnetization of one pole for the 10-12 PMSM

9-8 PMSM   The harmonic analysis of the flux waveform leads to a spectrum in which appears H_3, H_5, H_{12} and H_{14} (figure 13).
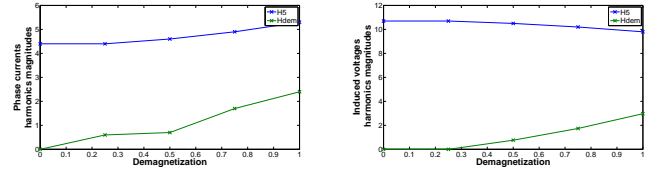

Fig. 11. Evolution of phase currents and induced voltages fundamental harmonic H5 and of demagnetization indicator Hdem with one pole demagnetization for the 10-12 PMSM.
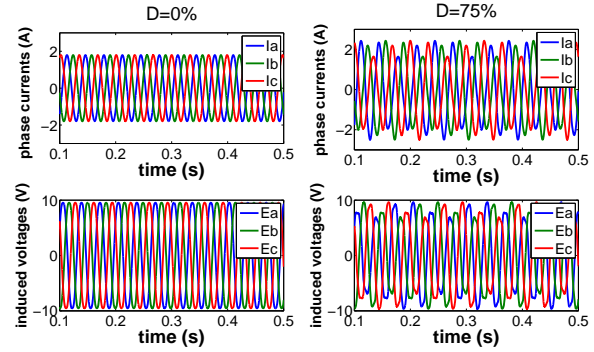

Fig. 12. Temporal evolution of the phase currents in case of demagnetization of one pole for the 9-8 PMSM
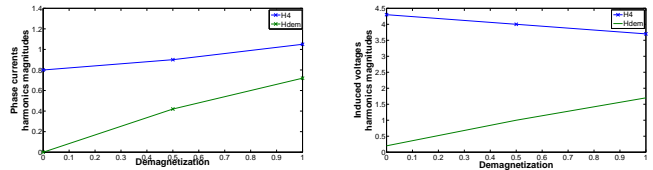

Fig. 13. Evolution of phase currents and induced voltages fundamental harmonic H4 and of demagnetization indicator Hdem with one pole demagnetization for the 9-8 PMSM.

H_{dem} indicator allows detecting and identifying one pole total or partial demagnetization for different stages of the fault.

5. TESTS

5.1 Short-circuits

In order to validate the model and the indicator choice, tests are run on short-circuited 9-slots 8-poles motors. The tested motors short-circuits are characterized by an unbalance indicator I_{unb} calculated from the phases resistance.

$$I_{unb} = \sqrt{\sum (R_x - R_x nom)^2}, x = a, b, c \qquad (15)$$

Phase resistance depends on the number of healthy and short-circuited turns and I_{unb} depends both on the number of spires and on the short-circuit resistance.

Simulations are run with this indicator (figure 14).

Several motors with several unbalance degrees are tested and phase currents are monitored (figure 15). Their short-circuit indicators Asc are computed and presented in figure 16.
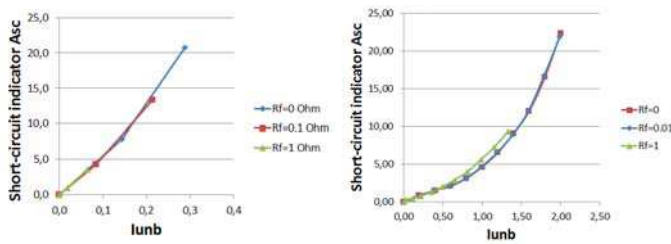
Fig. 14. Short-circuit indicator Asc as a function of unbalance indicator Iunb, for the 9-8 PMSM (left) and the 10-12 PMSM (right).
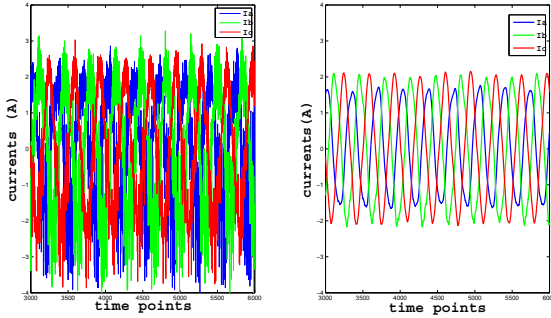

Fig. 15. Test result for a short-circuited motor (Iimb=0.3). Sensors output (left) and filtered signals (right). Test configuration is: phase to phase voltage max is 22V, mechanical speed is 450 rpm, acquisition frequency is 10kHz.
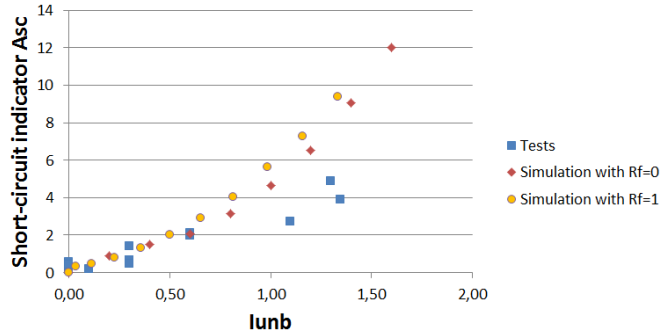

Fig. 16. Short-circuit indicator Asc variation as a function of unbalance indicator Iunb for the 9-8 PMSM.

Tests on short-circuited motors show results that are similar to the one obtained with the short-circuit model. A_{sc} increases with the short-circuit gravity.

5.2 Comparison between short-circuits and demagnetization consequences

In case of pole demagnetization without short-circuit A_{sc} remains equal to zero since there is no change in phase shift. This means that the proposed indicator is not affected by demagnetization, it is specific to inter-turns short-circuits. In case of short-circuit, H_{dem} remains equal to zero since the harmonics induced by inter-turns short-circuit are not the same. This indicator is specific to one pole partial or complete demagnetization.

Consequences of the two faults are very different which allows easy discrimination between them. It must be noticed that, in order to perform FDI, specific fault indicators have been built using available signals only (phase currents and rotor vs stator angular position). This is a great advantage for this kind of embedded application in term of cost and weight while others works [Penman][Casadei] design FDI systems with the help of electromagnetic flux sensors that is uneasy to implement on-board aircrafts.

6. CONCLUSION

The reported work is the design of a Fault Detection and Isolation system for an innovative 12-slots 10-poles synchronous machine and 9-8. The two most critical faults occurring on this machine have been identified as inter-turns short-circuits and rotor pole demagnetization. Nominal and faulty models have been developed. Analytical studies and simulation have provided a rich meant to identify the specific indicators for each fault. Unlike former studies that designed FDI systems with the resort to flux sensors that cannot be installed on- board, the proposed indicators only involve the available signals that are already used by the motor controller: phase currents and rotor vs stator position. The proposed supervision system will be completed soon with an additional module, the prognosis module, which will predict the remaining useful life of our motor.

REFERENCES

Cardoso, A.J.M., Cruz, S.M.A., and Fonseca, D.S.B. (1999). Inter-turn stator winding fault diagnosis in three-phase induction motors by park's vector approach. *IEEE Transactions on Energy Conversion*, 14(3).

Casadei, D., Filippetti, F., Rossi, C., and Stefani, A. (2009). Magnet fault characterization for permanent magnet synchronous motors. In *IEEE International Symposium on diagnostics for Electric Machines, Power Electronics and Drives*.

Farooq, J.A. (2008). *Etude du probleme inverse en electromagnetisme en vue de la localisation des defauts de desaimantation dans les actionneurs a aimants permanents.* Ph.D. thesis, Universit de technologie de Belfort-Montbelliard.

Khov, M. (2009). *Surveillance et diagnostic des machines synchrones aimants permanents : detection des courts-circuits par suivi parametrique.* Ph.D. thesis, Universit de Toulouse.

Nierlich, F. (2010). More electrical actuation for ata 32 : Modular power electronics and electrical motor concepts. In *SAE International*.

Penman, J., Sedding, H.G., and Fink, W.T. (1994). Detection and location of interturn short circuits in the stator windings of operating motors. *IEEE Transactions on Energy Conversion*, 9(4).

Ruschetti, C., Bossio, G., and Angelo, C.D. (2010). Effects of partial rotor demagnetization on permanent magnet synchronous machines. In *IEEE International Conference on Industrial Technology (ICIT)*.

Trigeassou, J.C. (2011). *Diagnostic des machines electriques.* Lavoisier.

Vaseghi, B. (2009). *Contribution a l'etude des machines electriques en presence de defauts entre spires - modelisation, reduction du courant de defaut.* Ph.D. thesis, Institut National Polytechnique de Lorraine.